Ancient TL

Decomposition of UV induced ESR spectra in modern and fossil dental enamel fragments

R. Joannes-Boyau and R. Grün

Research School of Earth Sciences, The Australian National University, Canberra, ACT 0200, Australia (e-mail renaud.joannes-boyau@anu.edu.au)

_____

Abstract
Using an automated simulated annealing (SA) procedure, spectrum decomposition on angular measurements of tooth enamel fragments shows that UV irradiation of modern human and fossil bovid samples results in distinctively different ESR spectra. In the fossil sample, UV irradiation generates qualitatively identical spectra to natural. The amounts of non-oriented CO_2^- radicals in the modern and fossil samples are about 35% and 9%, respectively. The two oriented CO_2^- radicals, R_1 and R_2, attributed to orthorhombic and axial types, show a ratio of 64:36 in the modern and 34:66 in the fossil sample. R_1 is also observed in the natural fossil sample, while the axial type was either absent or too small to be identified in a γ-irradiated fossil sample. We could not observe a measurable UV induced signal after 7 months of sunlight and laboratory light exposure, respectively. The clear difference between γ and UV induced signal raises the possibility of using UV lights for dating protocols.

Introduction
Radiation induced signals in tooth enamel can be used for the evaluation of past radiation doses in retrospective dosimetry (e.g. Ikeya et al. 1984; Romanyukha et al. 1994), and dating (e.g. Grün, 1989, Grün et al. 2008). These two application areas differ with respect to the dose ranges evaluated and the age of the materials. While retrospective dosimetry deals with a dose range from a few mGy to 5 or 10 Gy on modern teeth, dating deals with old teeth (usually between several thousand and up to several million years old) and a dose range from a few Gy to several thousands of Gy. The radiation induced signals in fossil teeth are qualitatively different from those of modern teeth as any unstable signals in fossil teeth have partly or completely faded over geological times.

Previous studies suggested that the main ESR signal generated by gamma radiation can be attributed to two categories of CO_2^- radicals, one anisotropic (AICOR) and the other with no preferential orientation, also called non-oriented CO_2^- radicals (NOCOR) (e.g. Callens et al. 1995; Brik et al. 2000; Ishenko et al. 2002; Grün et al. 2008; Joannes-Boyau and Grün, 2009). In fossil teeth it was found that 9% of NOCORs were present in the natural sample, while 40% were present in the laboratory γ-irradiation component (Joannes-Boyau et al. in press, submitted). Those values differ from modern teeth, which have up to 80% NOCORs after γ-irradiation (Vorona et al. 2007; Rudko et al. 2007). However, the calculation method used for these studies differs from ours which could lead to systematic errors. Two studies by Joannes-Boyau et al. (in press, submitted) demonstrated that two types of AICORs (axial and orthorhombic) contribute to the ESR signal of fossil tooth enamel. In the γ-induced spectra, the axial form (R_2) was undetected (either absent or negligible) and only the orthorhombic form (R_1) contributed to the anisotropic ESR spectral components (Joannes-Boyau et al. in press).

Studies on retrospective dosimetry suggested that UV may contribute significantly to the overall ESR intensity (Liidja et al. 1996; Nilsson, 2001; El-Faramawy 2005). Brik et al. (1998) and Vorona et al. (2007) showed that UV induced spectra in modern teeth contained significantly less NOCORs than those by γ-irradiation. However, the relative depletion of NOCORs could have been the result of a combination of UV radiation and heating during the experiment. UV exposure is usually associated with significant heating but it is not known whether samples were cooled during these experiments. The occurrence of methyl radicals in the ESR spectra of Nilsson (2001) indicates a possible thermal influence, but these radicals could have been induced by UV irradiation itself.

The aim of the present study was to assess the influence of UV light on fossil teeth enamel, focusing particularly on dose estimation.
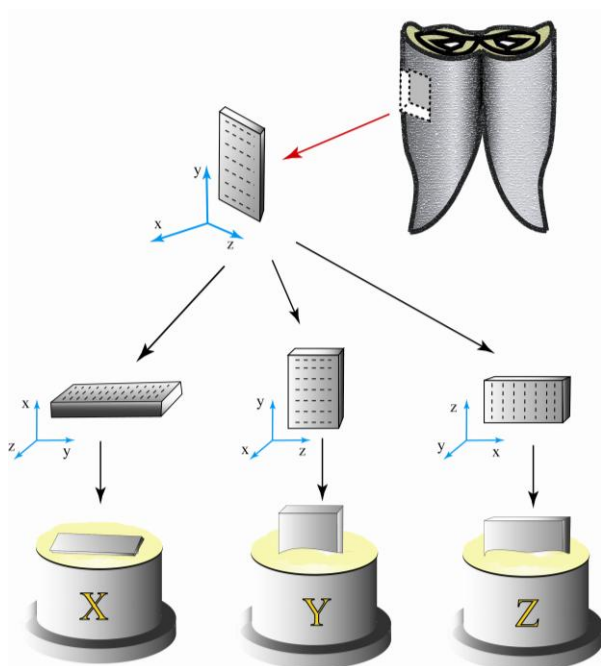
Figure 1: *Direction of axes and configurations used for the measurement of the tooth enamel fragment (from Joannes-Boyau and Grün 2009).*

Materials and methods

The experiments were carried out on a tooth enamel fragment of a modern human (to avoid ethical problems, one of our own teeth was analysed) and on a fossil bovid from the archaeological site of Holon estimated at around 200,000 years old (for more details see Porat et al. 1999). A long lamella was separated from the fossil tooth (H2) using a dental diamond saw and a series of consecutive fragments were extracted and used for a range of heating and irradiation experiments (e.g. Grün et al. 2008; Joannes-Boyau and Grün 2009; Joannes-Boyau et al. in press, submitted). The modern human sample (MH) was used to validate the modus operandi for the Holon study and to compare results with previous studies conducted by Liidja et al. (1996), Nilsson et al. (2001), El-Faramawy (2005), Vorona et al. (2007) and Rudko et al. (2007).

The methodology established by Joannes-Boyau et al. (in press, submitted) was used for the present study. X, Y and Z denote configurations, x, y and z, the main axes of the measured fragment (Fig. 1). T1, B1 and B2 are positions in the measured or simulated ESR spectra, and R_1, R_2, R_3 and B_2 the fitted Gaussian components (for more details see Joannes-Boyau et al., submitted). The concentrations for the radicals were derived from the double integration of the fitted lines to account for changes in the line width. For the features in the measured ESR spectra,

T1-B1 and B2, it was not possible to carry out double integrations; their angular variations were derived from their intensities (for more details see Joannes-Boyau et al., in press, submitted).

Both fragments H2 and MH were each mounted in three separate Teflon holders containing a Parafilm mould and were incrementally measured by rotating them around their three major axes. We used the following configurations: X: rotation around the axis perpendicular to the dentine-enamel junction, Y: around the axis of tooth growth and Z: perpendicular to X and Y (Fig. 1). The sample holders were inserted in a Bruker ER 218PG1 programmable goniometer and measured with a Bruker Elexys E500 ESR spectrometer in 10° increments over 360° with the following measurement conditions: 2 mW microwave power, 0.1 mT modulation amplitude 12 mT sweep width with a sweep time of 21 s. The spectra were accumulated over 50 consecutive measurements. The sample was measured before and after irradiation.

The fragments were exposed to UV light for 168 hours using a Hoenle UVASPOT 400T lamp emitting UVA/B at 400 W producing incident energy of 5.05 ± 0.1 mW cm^{-2} at the sample location. The temperature was recorded in 2 min intervals with a thermolog controller near the surface and at the base of the fragments, located near the cooling plate. The measured temperatures were $21 \pm 2 °C$ at the base of the sample and $33 \pm 2 °C$ at the top. The γ-irradiation was carried out with a ^{137}Cs-source for 100 min, which corresponds to an approximate dose of 187 Gy (the experiment is described in Joannes-Boyau et al., in press).

Extraction of the isotropic components of the UV induced spectra

The first step in spectra decomposition of H2 consists of subtracting the natural signal from the UV irradiated spectra. The alignment of the two spectra is the key to avoid artefact signals, for that matter the isotropic methyl lines are used as markers for alignment. Previous studies by Joannes-Boyau et al. (in press, submitted) have shown that non-CO_2^- components are found in the natural signal and in the irradiated signal (Fig. 2a). Those signals described as isotropic lines have to be removed before decomposing the ESR spectrum at each angle. In the fossil sample, the isotropic lines in the UV-induced spectra were found to have a similar signature as in the natural (combined into one signal, named Isotropic Combined signal (IC)) (Fig. 3), but increased with UV exposure. No methyl line was created by UV exposure. A wide line, W_2, at g=2.0051 (see Joannes-Boyau et al. submitted),

Figure 3*: Comparison of the isotropic signal found in the modern and fossil tooth natural spectra IC (from Joannes-Boyau et al., submitted) (a), fossil tooth UV irradiation spectra (b), modern human tooth UV irradiation spectra (c) and modern human tooth natural spectra (d) respectively. The symbol $ indicates the unknown isotropic line that appears with UV exposure described in the text with a g-value around g=2.0093.*
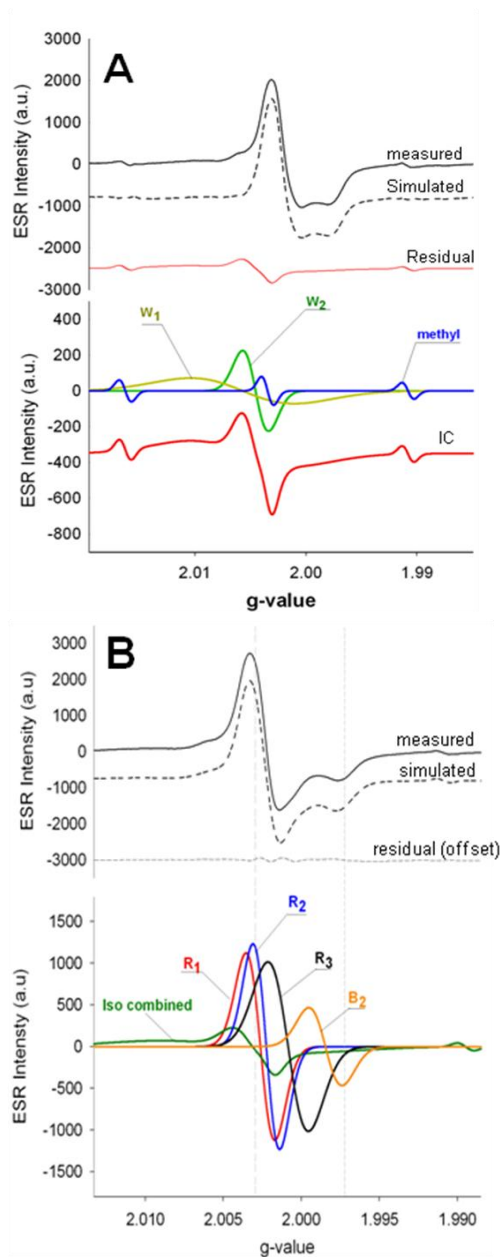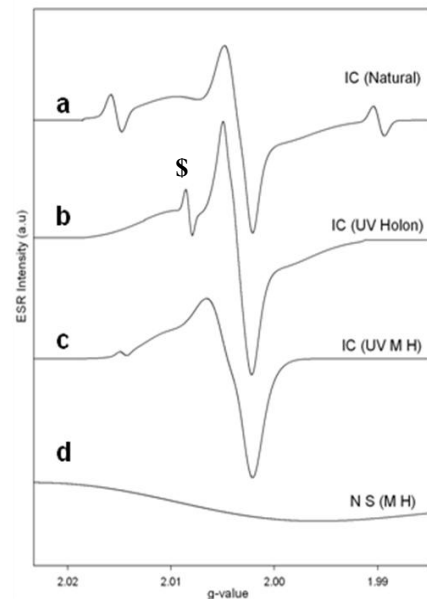
Figure 2: *Decomposition of the measured spectra (for more details see Joannes-Boyau et al. in press). A: (Top) Isotropic lines in the natural spectra. A simulated signal is fitted into the natural measured spectra to extract the isotropic component (IC is the residual offset for clarity). (Bottom) Position of the isotropic components that when merged form the Iso-combined spectra (IC). B: (Top) Comparison of the measured and simulated spectra. The residual is offset for clarity and corresponds to the subtraction of the simulated spectra from the measured. (Bottom) Decomposition of the measured spectra using the SA decomposition with four Gaussian components representing the anisotropic lines R_1, R_2, R_3 and B_2.*
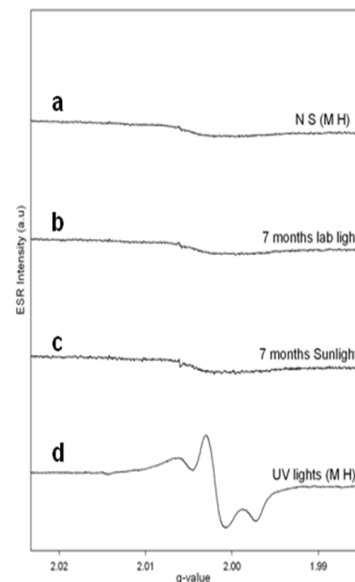

Figure 4: *Comparison of the influence of different exposure on the merged ESR signal of modern human tooth enamel fragment. (a) Native signal N.S.; (b) 7 months laboratory lights (c) 7 months sunlight exposure (d) 168 hours UV lamp exposure.*

attributed to a combination of SO_2^- and CO^- radicals, increased. SO_2^- radicals which occur at g=2.0056 are most likely responsible for this increase (Bouchez et al. 1988; Schramm and Rossi 1999, see also the fitting of Grün 2002). The SO_2^- radical is known to be temperature sensitive. It is likely that the SO_2^- radicals were created at the surface of the sample where the temperatures were slightly higher due to the UV exposure. A new isotropic line ($) at g=2.0093, with a line width of around 0.1 mT (Fig. 3) was created by UV radiation. This new, unknown component does not interfere with the main signal and fades rapidly (its intensity is negligible after three months storage at ambient temperature). The NOCORs were removed using the same amount found in the natural signal corresponding to 9% of the total intensity. After subtracting all aforementioned components (natural, isotropic lines and NOCORs), only UV-induced anisotropic components remain.

Spectrum Decomposition

The anisotropic components of the irradiation spectra were decomposed with an automated simulated annealing (SA) procedure which is particularly well suited to separating overlapping signals (Fig. 2b) (for more details see Joannes-Boyau et al. in press, submitted). SA is a Monte Carlo method used for combinatorial optimisation problems (for details see Metropolis et al. 1953; Kirkpatrick et al. 1983; Černý 1985; Mossegard and Sambridge 2002; Bodin and Sambridge, 2009). The spectra were decomposed with four Gaussian lines which had the same prescribed g-value range limits used in the previous study to avoid unrealistic solutions outside the regions for the CO_2^- radicals in hydroxyapatite (see above). No restrictions were set on the intensity although the line widths were kept between 0.10 mT and 2 mT to avoid aberrations. Our SA procedure is able to randomly generate a large number of synthetic spectra defined by a linear combination of four Gaussian lines. Each simulated spectra is compared to the measured spectra in terms of a least square misfit.

Results and discussion

The modern human tooth (MH) contains a wide, isotropic signal centred at 2.0044 ± 0.0005 prior to any irradiation, also called the native signal (NS) (Liidja et al. 1996; see Figs. 3 and 4). Due to the intensity and width of the signal compared to the background, the measured g-value is not very precise. The spectra confirm that the enamel fragment was not exposed to any measurable ionising radiation. The ESR spectra after 168 hours UV exposure is qualitatively different from the natural, as the shapes of the two spectra clearly differ (Fig. 4).

(a)

(b)

(c)

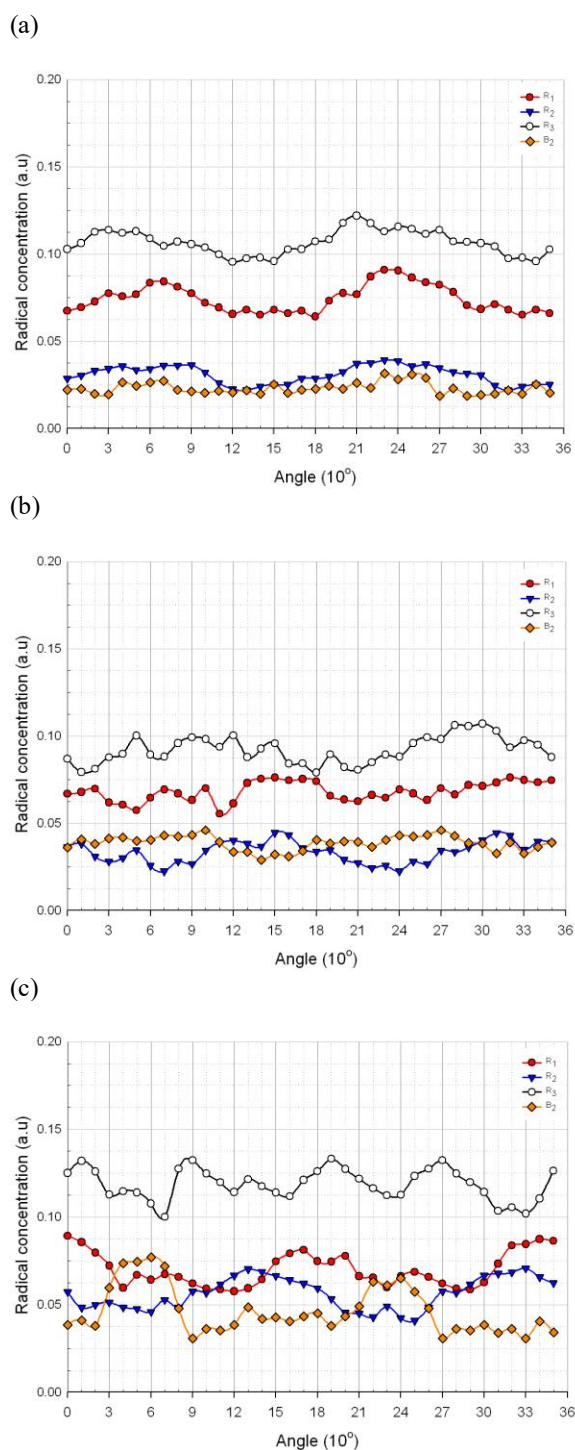**Figure 5**: *Angular variation of ESR signals induced by UV exposure in a modern human fossil tooth enamel fragment. Summary of all decomposition results of the radical concentration (obtained by double integration) variation over 360° (a) X-configuration, (b) Y-configuration and (c) Z-configuration of R_1, R_2, R_3 and B_2 component. Note that on the Z-configuration R_3 shows a 90° symmetry.*

	Minimum g-value	Angle (°)	Maximum g-value	Angle (°)	Minimum width (mT)	Angle (°)	Maximum width (mT)	Angle (°)	Minimum radical conc.	Angle (°)	Maximum radical conc.	Angle (°)	Angular Variation	Average radical conc.	Relative radical conc. (%)
Z-configuration															
R_1	2.0026	190	2.0030	270	0.42	240	0.42	190	0.06	100	0.09	0	0.45	0.07	24.0
R_2	2.0019	70	2.0025	210	0.26	140	0.30	260	0.04	250	0.07	330	0.53	0.06	19.3
R_3	2.0005	230	2.0008	10	0.46	90	0.54	140	0.10	70	0.13	190	0.28	0.12	40.8
B_2	1.9984	30	1.9987	240	0.30	320	0.34	190	0.03	330	0.08	60	1.01	0.05	15.9
Y-configuration															
R_1	2.0026	190	2.0030	300	0.36	220	0.44	30	0.06	230	0.08	320	0.30	0.07	29.3
R_2	2.0020	250	2.0025	110	0.24	100	0.36	0	0.02	240	0.04	150	0.66	0.03	14.4
R_3	2.0006	240	2.0008	320	0.45	170	0.54	80	0.08	180	0.11	300	0.30	0.09	39.6
B_2	1.9983	50	1.9985	310	0.28	220	0.34	120	0.03	140	0.05	270	0.44	0.04	16.7
X-configuration															
R_1	2.0026	170	2.0029	270	0.32	320	0.42	60	0.06	170	0.09	230	0.36	0.07	31.6
R_2	2.0022	170	2.0025	100	0.26	90	0.36	160	0.02	160	0.04	230	0.56	0.03	13.1
R_3	2.0006	100	2.0009	240	0.47	230	0.54	150	0.10	120	0.12	210	0.25	0.11	45.4
B_2	1.9983	220	1.9986	140	0.31	150	0.35	80	0.02	270	0.03	230	0.55	0.02	9.8

Table 1: *Results of the decomposition of the anisotropic components of the modern tooth after UV-irradiation*

The native signal grows slightly with irradiation, at the same time that CO_2^- radicals appear in the spectra. Subtracting the native signal (multiplied by a factor 1.2) plus an isotropic component (IC MH in Fig. 3) which is similar to the one used in the natural sample from Holon (IC Natural, see Joannes-Boyau et al., submitted), yields typical CO_2^- radicals. The amount of NOCORs is around 35%.

Fig. 5 and Table 1 summarise the angular response of the four UV generated Gaussian components in MH. We observe an overall R_1:R_2 ratio of 64:36. The maxima and minima of R_1 and R_2 in the various configurations are offset by 0°, 0° and -30° in X, Y and Z-configuration, respectively, indicating different orientations of the radicals within the crystal structure. Similar values were found by Joannes-Boyau and Grün (2009) in the sample from Holon with offsets of -26°, 7° and -5° ± 10° in X, Y and Z-configurations, respectively. The angular differences between R_1 and R_2 of the two teeth point to differences in the tooth formation of the two species.

The results obtained on MH are similar to those described in the literature (e.g. Callens et al. 1995, 1998; Liidja et al. 1996; Nilsson et al. 2001; El-Faramawy 2005; Vorona et al. 2007; Rudko et al., 2007). The exception is that no methyl radicals were found in our measurements, contrary to Nilsson et al. (2001). This makes us confident that temperature was well controlled by the cooling plate used in the present study and that the anisotropic signal extracted from the fossil tooth is UV rather than temperature induced. After 3 months, the UV induced spectra show major changes. The NOCORs have faded by 15% of their intensity but still represent 30% of the initial spectra. The T1-B1 region is slightly shifted to higher g-values and shows a depletion of 3 to 5% of its original signal. The ratio between R_1:R_2 has changed to 59:41 respectively. The ratio disparity after 3 month could be attributed to the disappearance of some of the R_1 species and at the same time the appearance of new R_2 radicals. However, because of the small amount of variation (between 3 to 5%), we cannot conclude that any transfer process took place within the 3 months.

The fossil bovid tooth
In Z-configuration the angular variations of the natural and UV spectra show little difference while those of the γ-spectra are significantly muted (Fig. 6). This can be attributed to the much higher contribution of the NOCORs in the γ-component (around 40%) compared to the natural (around 9%, see Joannes-Boyau et al. in press). This also implies that the relative distributions of the NOCORs in the natural and UV components are approximately the same; otherwise the angular variation would change dramatically such as the γ-induced variation, since NOCORs remains constant at all angles (see Joannes-Boyau et al., in press).

Fig. 7 compares a natural spectrum to those of the γ- and UV components. While it is not possible to scale the natural spectrum to fit the γ-component (Fig. 7a), due to a distinctively different distribution of AICORs (Joannes-Boyau et al, in press), the natural spectrum can be easily scaled into the UV component (Fig. 7b). This implies a closely similar distribution of the different types of CO_2^- radicals in the natural and UV components. Scaling the natural spectrum by a factor of 1.75 into the natural + UV, leaves small residuals with signal intensities of 5.6%, 5.0% and 4.4% in X, Y and Z configuration, respectively (Fig. 8). These residuals are approximately the same as when using multi-component decompositions of spectral components (Joannes-Boyau et al. in press, submitted).
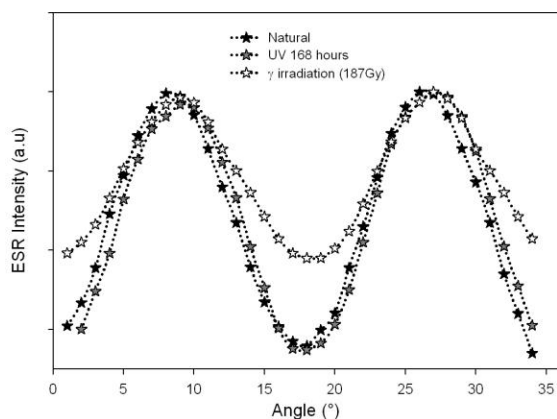
Figure 6: *Angular variation of the natural, UV induced and γ-induced spectra in Z-configuration on fossil tooth enamel fragments.*

		T1-B1	B2
Natural	Z	0.6	0.74
	Y	0.62	0.53
	X	0.31	0.4
Natural+γ	Z	0.44	0.39
	Y	0.43	0.23
	X	0.17	0.17
Natural+UV	Z	0.61	0.71
	Y	0.61	0.51
	X	0.30	0.43
Natural (anisotropic)	Z	0.66	0.79
	Y	0.68	0.57
	X	0.33	0.43
γ (anisotropic)	Z	0.76	0.57
	Y	0.78	0.51
	X	0.45	0.46
UV (anisotropic)	Z	0.67	0.75
	Y	0.66	0.54
	X	0.37	0.46

Table 2: *Angular variation*

Fig. 9 shows the stacks of all spectra of the anisotropic components of the natural sample as well as of the UV and γ-induced (see also Tables 2 to 4). The γ-irradiation stacks, especially the Y-configuration, show a very different pattern to the corresponding UV stacks (Fig. 8, middle column, rows B and C). The T1-B1 complex is significantly narrower in the γ-irradiation spectra than in the other two. The angular variations of the T1-B1 and B2 positions (marked in Fig. 6) of the γ-irradiation spectra are significantly more pronounced in all configurations than of the natural and UV spectra (Table 5). At the same time, it is unclear why UV exposure induces a smaller amount of NOCORs than γ-irradiation. Perhaps this is due to the energy difference between UV emissions (in the range of 3 to 10 eV) and γ rays (>600 keV). So far no explanation can be clearly proposed, however, local saturation of radicals could induce significant differences in the signals.
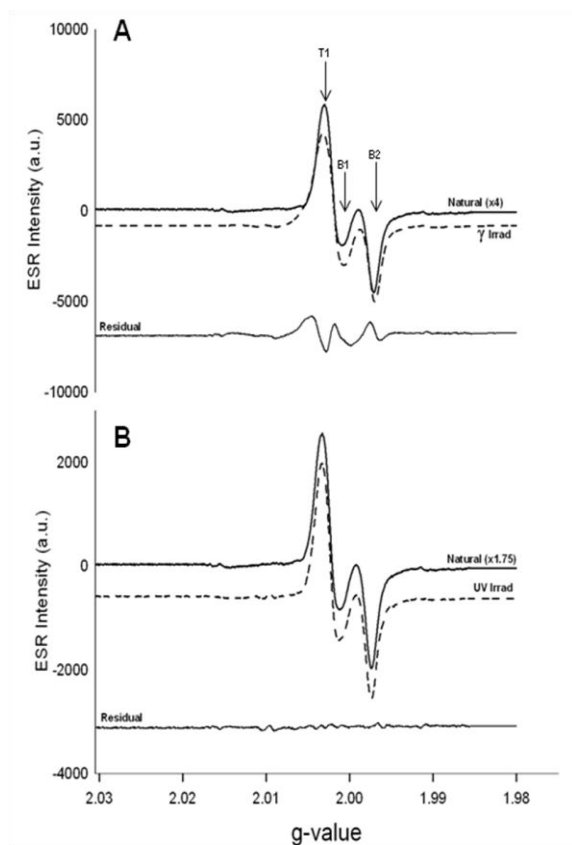

Figure 7: *Comparison of γ and UV irradiation influence on the ESR spectra of fossil bovid enamel fragment. The residual shows that γ-irradiation creates a completely different signal than the natural while the UV irradiation only modifies quantitatively the spectra of the Z-configuration.*

Fig. 10 and Tables 2 to 4 summarise the results of the decomposition. Note that the R_2 component was not identifiable in the γ-irradiation spectra (Joannes-Boyau et al. in press) while it is present in both natural and UV spectra. The g-values of the four components are in a similar range and do not show any significant shifts for the natural and UV irradiated signals. Their line widths appear slightly narrower in UV than in the natural, but this parameter always shows the largest deviations in repeated SA runs (Joannes-Boyau et al. submitted). The average and relative radical concentrations of natural spectra
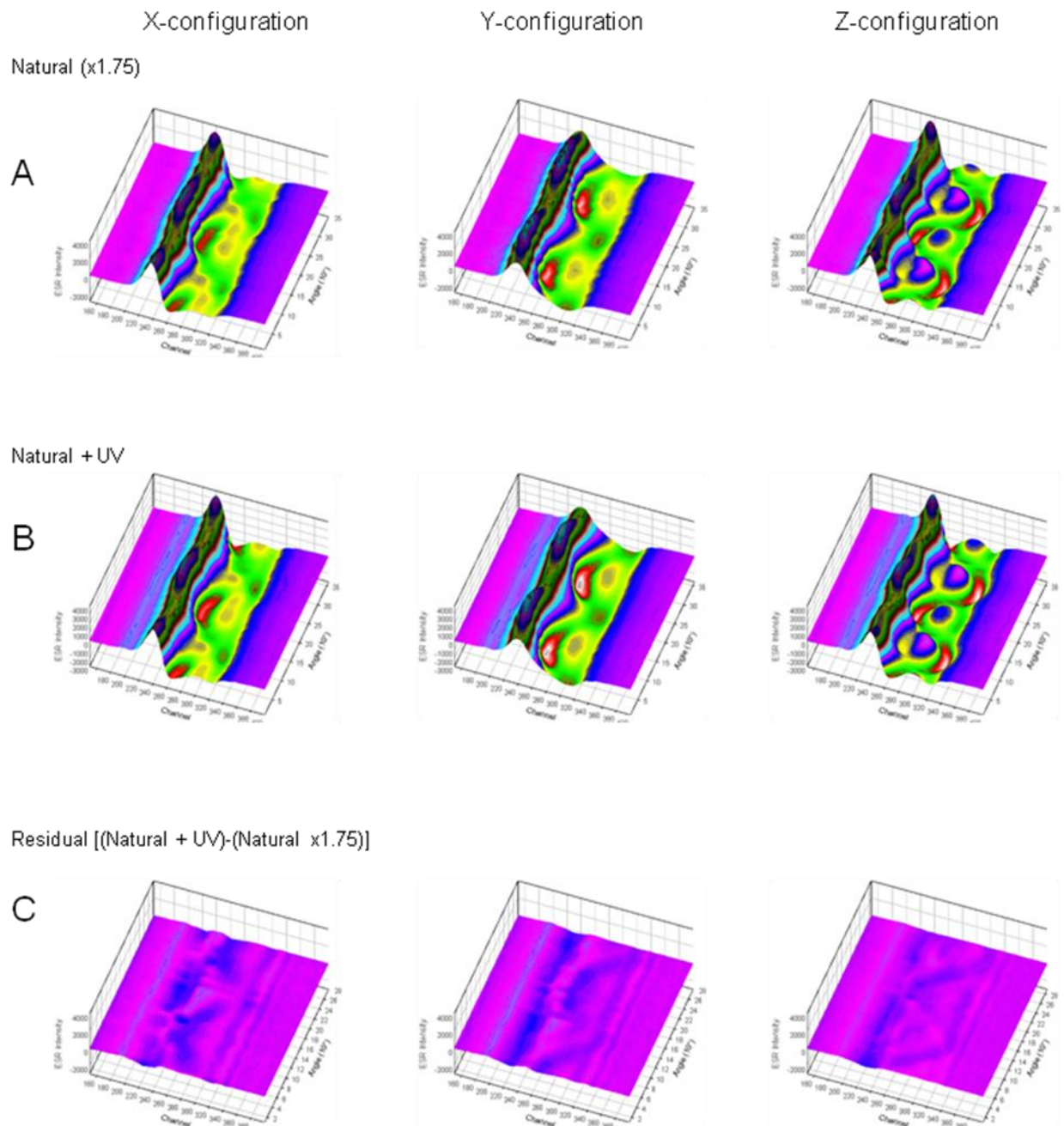
Figure 8*: Stacks of fossil bovid enamel natural spectra multiplied by a factor of 1.75 (row A), natural + UV irradiation (row B) and residual from the subtraction of the natural (x1.75) from the natural + UV irradiation (row C) for the three configurations X, Y and Z, column 1, 2 and 3 respectively.*
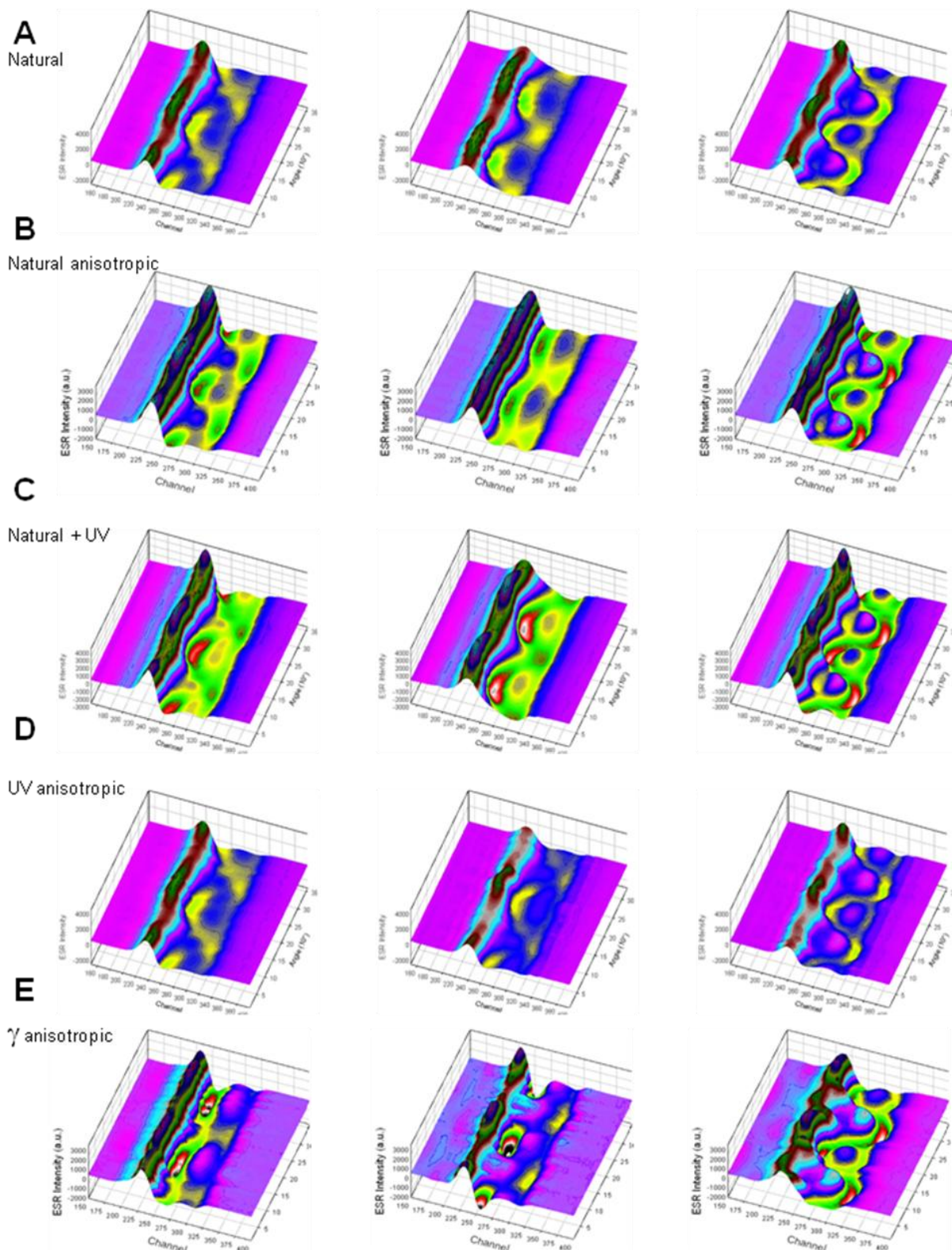
Figure 9: *Stacks of fossil bovid enamel: natural spectra (row A), natural anisotropic (row B), natural + UV irradiation (row C), UV exposure anisotropic spectra (row D) and γ-irradiation anisotropic spectra (row E) for the three configurations X, Y and Z, column 1, 2 and 3 respectively.*
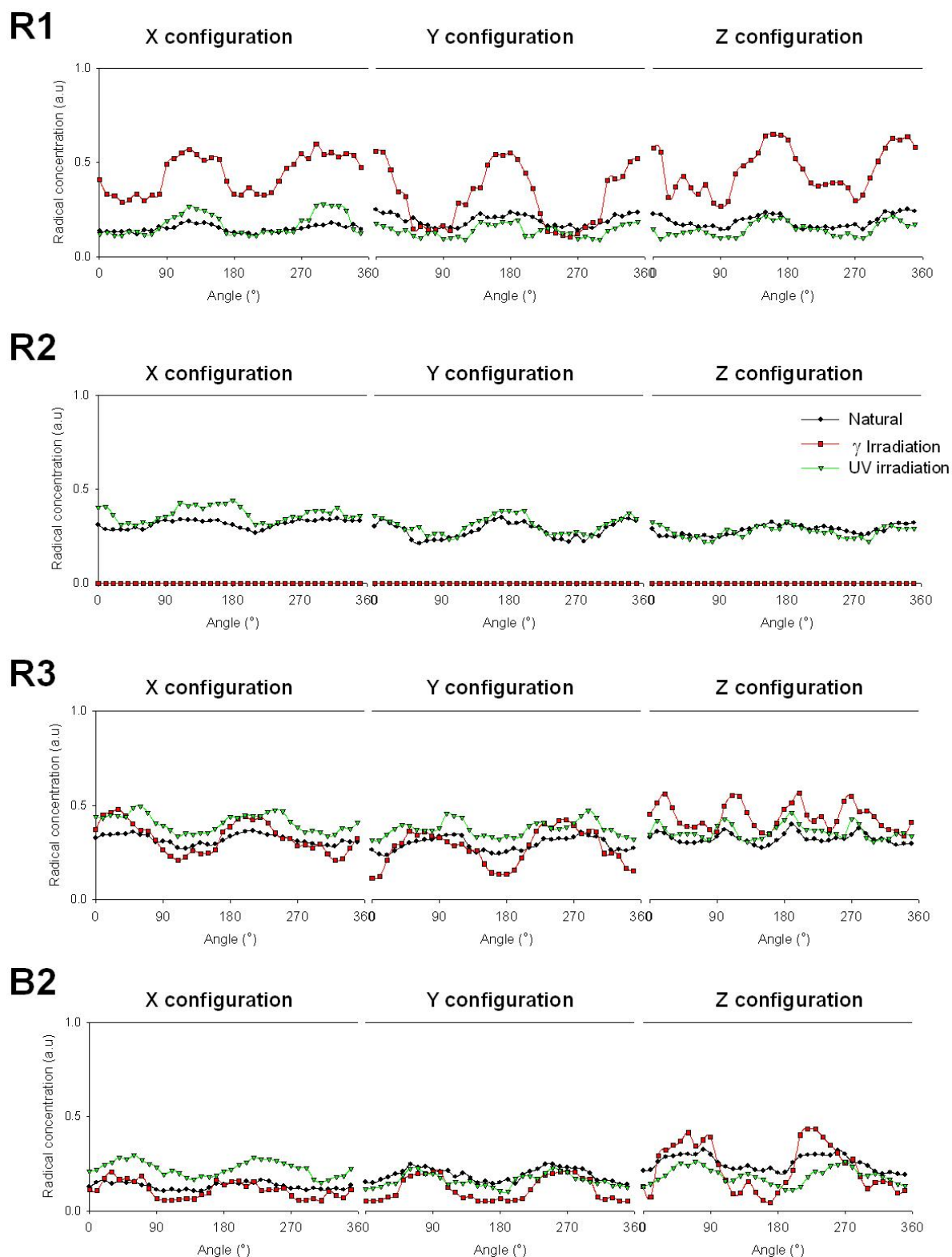
Figure 10: *Summary of the angular behaviour of the anisotropic components of the natural spectra as well as the UV irradiation spectra decomposed with four Gaussian components and with the γ-irradiation spectra decomposed with three Gaussian components (see Joannes-Boyau et al., in press).*

	Minimum g-value	Angle (°)	Maximum g-value	Angle (°)	Minimum width (mT)	Angle (°)	Maximum width (mT)	Angle (°)	Minimum radical conc.	Angle (°)	Maximum radical conc.	Angle (°)	Angular Variation	Average radical conc.	Relative radical conc. (%)
Z-configuration															
R_1	2.0026	170	2.0029	250	0.26	150	0.32	50	0.14	30	0.33	170	0.64	0.22	14.6
R_2	2.0019	120	2.0024	240	0.31	50	0.39	300	0.38	290	0.55	180	0.31	0.46	30.6
R_3	2.0005	190	2.0010	300	0.39	100	0.51	190	0.47	150	0.70	210	0.58	0.55	36.1
B_2	1.9980	330	1.9989	250	0.29	210	0.42	80	0.17	20	0.40	70	0.57	0.28	18.7
Y-configuration															
R_1	2.0026	20	2.0029	300	0.26	0	0.33	110	0.14	120	0.29	190	0.62	0.23	13.9
R_2	2.0018	220	2.0023	250	0.36	220	0.39	100	0.36	110	0.59	200	0.40	0.47	31.5
R_3	2.0004	280	2.0010	10	0.40	180	0.51	240	0.48	10	0.72	250	0.42	0.57	38.1
B_2	1.9984	270	1.9989	150	0.31	260	0.42	310	0.16	190	0.34	290	0.62	0.25	16.5
X-configuration															
R_1	2.0026	240	2.0028	330	0.27	130	0.30	240	0.27	150	0.52	250	0.49	0.28	15.6
R_2	2.0019	170	2.0024	280	0.36	240	0.41	180	0.47	160	0.63	110	0.20	0.51	28.5
R_3	2.0005	190	2.0009	320	0.41	120	0.54	20	0.51	70	0.75	20	0.39	0.62	34.6
B_2	1.9984	100	1.9989	200	0.33	250	0.42	40	0.26	250	0.50	0	0.53	0.38	21.1

Table 3: *Results of the decomposition of the anisotropic components in the UV spectra*

	Minimum g-value	Angle (°)	Maximum g-value	Angle (°)	Minimum width (mT)	Angle (°)	Maximum width (mT)	Angle (°)	Minimum radical conc.	Angle (°)	Maximum radical conc.	Angle (°)	Angular Variation	Average radical conc.	Relative radical conc. (%)
Z-configuration															
R_1	2.0025	190	2.0027	210	0.28	330	0.35	110	0.28	110	0.50	330	0.58	0.38	17.7
R_2	2.0020	280	2.0024	60	0.36	190	0.42	300	0.50	50	0.65	180	0.26	0.58	27.0
R_3	2.0003	80	2.0006	160	0.39	90	0.47	180	0.51	150	0.82	170	0.47	0.65	30.2
B_2	1.9982	230	1.9987	10	0.33	230	0.42	0	0.43	350	0.65	80	0.41	0.54	25.1
Y-configuration															
R_1	2.0026	80	2.0028	350	0.27	170	0.32	280	0.22	80	0.48	0	0.54	0.36	18.2
R_2	2.0019	110	2.0023	350	0.38	110	0.42	320	0.42	60	0.66	170	0.41	0.57	28.8
R_3	2.0004	270	2.0006	110	0.41	130	0.48	310	0.56	20	0.74	280	0.28	0.65	32.8
B_2	1.9985	320	1.9988	100	0.36	70	0.42	300	0.30	340	0.52	80	0.54	0.40	20.2
X-configuration															
R_1	2.0026	20	2.0028	150	0.27	150	0.31	260	0.22	210	0.39	120	0.43	0.29	14.9
R_2	2.0020	20	2.0023	290	0.41	110	0.42	280	0.60	210	0.72	290	0.18	0.67	34.5
R_3	2.0003	110	2.0006	200	0.47	130	0.54	300	0.62	120	0.77	210	0.22	0.69	35.6
B_2	1.9984	130	1.9987	220	0.39	70	0.42	300	0.19	140	0.38	230	0.49	0.29	14.9

Table 4: *Results of the decomposition of the anisotropic components in the natural spectra*

are somewhat different to the UV induced (compare Table 2 with 3). The angular variations for all components of UV spectra were slightly higher than the natural, but were smaller than the γ-irradiation spectra (compare Tables 2, 3 and 4). This clearly implies that UV radiation causes a significantly different radical distribution in the enamel than γ-irradiation. The fading observed on the UV irradiated signal for modern human tooth after three months is not as evident for the fossil bovid tooth. The difference in signal intensity between the last UV exposure and the fading test conducted 3 months later is in the range of 3 to 4% of the total intensity. Prima facies, it appears that the diminution is induced by the fading of some NOCORs. However, the spectra depletion falls into the error range and therefore does not allow any affirmation.

Average R_1:R_2 ratios in natural and UV components are different in the three configurations (compare Tables 2 and 3). Nonetheless, when normalising on the total radical concentration, R_1:R_2 in the natural (35:65) is virtually the same as the UV ratio (34:66).

Based on the ESR intensity of the fragment, we have estimated that the UV lamp is the γ-equivalent of 3.1 ± 0.3 mGy/min. Since the natural and UV spectra show closely similar radical distributions (in contrast to γ-irradiation), UV irradiation could be more suitable than γ-irradiation for the establishment of dose response curves in ESR dating. While fading, unknown intensity attenuation and energy calibration will complicate this approach at the present time, systematic correlations between UV exposure and the equivalent dose from γ-irradiation could lead to the use of photons instead of γ-rays for dating purposes. Further, studies should be undertaken on the effect of UV on the equivalent dose (D_e) assessment, however, because UV irradiation is a very slow process, local saturation could happen during exposure. For that reason, a specific protocol should be designed to measure the sample while irradiating, which would complicate the experiment greatly.

The high radical concentrations induced by UV raise the possibility that sunlight or laboratory light induced radicals may interfere with dose estimations.

However, intermittent exposure to daylight for more than 50 years while laughing about ones own bad jokes did not induce any measurable CO_2^- radicals in MH, neither did exposure to indirect sunlight or laboratory light over 7 months in the fossil sample (Fig. 4). Samples are normally shielded behind window glass, known to block UV, and it is therefore unlikely that archaeological samples are exposed to direct UV sunlight over extended periods of time.

Summary
UV and γ-irradiation induce very different compositions of CO_2^- radicals in tooth enamel. In a modern sample, UV generated 35% of NOCORs and a mix of 64:36 of orthorhombic to axial radicals. In the fossil sample, UV generated 9% NOCORs and a mix of 34:66 of orthorhombic to axial radicals. While there are some differences between the natural and UV components in the various configurations, the overall radical distribution of the UV and the natural is the same. This is in contrast to γ-irradiation component of the fossil sample, which had about 40% AICORs and no axial radicals. While the UV components in the modern samples showed strong fading over three months (18 to 20% of the spectra) with possible transfer process between R_1 and R_2, the fading in the fossil sample was small (3 to 4%).

Blocked sunlight and laboratory light exposure over 7 months had no measurable influence on the samples.

Conclusions
Like γ-irradiation, UV irradiation induces significant differences between modern and fossil samples. While this change must have an impact on dose estimations, this aspect has never been systematically investigated in ESR dating. In the fossil sample, UV generates a similar mixture of CO_2^- radicals as found in the natural while the γ-irradiation response is completely different. This could make UV irradiation the choice for the establishment of dose response curves.

Acknowledgments

References
Bodin, T., Sambridge, M. (2009) Seismic tomography with the reversible jump algorithm. *Geophys. J. Int.* **178**, 1411-1436.

Bouchez, R., Cox, R., Hervé, A., Lopez-Carranza, E., Ma, J.L., Piboule, M., Poupeau, G., Rey, P. (1988) Q-Band ESR studies of fossil teeth: consequences for ESR dating. *Quaternary Science Reviews* **7**, 497-501.

Brik, A.B., Haskell, E.H., Scherbina, O.I., Brik, V.B., Atamanenko, O.N. (1998) Alignment of radicals of tooth enamel with heating. *Mineralogy Journal* **20**, 26–36.

Brik, A.B., Rosenfeld, L.G., Haskell, E.H., Kenner, G.H., Brik, V.B. (2000) Formation mechanism and localization places of CO2- radicals in tooth enamel. *Mineralogy Journal* **22**, 57-67.

Callens F., Moens P., Verbeeck R. (1995) An EPR study of intact and powdered human tooth enamel dried at 400°C. *Calcified Tissue International* **56**, 543–548.

Callens, F., Vanhaelewyn, G., Matthys, P., Boesman, E. (1998) EPR of carbonate derived radicals: applications in dosimetry, dating and detection of irradiated food. *Applied Magnetic Resonance* **14**, 235–254.

Černỳ, V. (1985) A thermodynamical approach to the travelling salesman problem: an efficient simulation algorithm. *Journal of Optimization Theory and Applications* **45**, 41-51.

El-Faramawy, N.A. (2005) Comparison of γ- and UV-light-induced EPR spectra of enamel from deciduous molar teeth. *Applied Radiation and Isotopes* **62**, 191–195.

Grün, R. (1989) Electron spin resonance (ESR) dating. *Quaternary International* **1**, 65-109.

Grün, R. (2002) ESR dose estimation on fossil tooth enamel by fitting the natural spectrum into the irradiated spectrum. *Radiation Measurements* **35**, 87-93.

Grün, R., Joannes-Boyau, R., Stringer, C. (2008) Two types of CO^{2-} radicals threaten the fundamentals of ESR dating of tooth enamel. *Quaternary Geochronology* **3**, 150-172.

Ikeya, M., Miyajima, S., Okajima, S. (1984) ESR dosimetry for atomic bomb survivors using shell buttons and tooth enamel. *Journal of Applied Physics* **23**, 697–699

Ishchenko, S. S., Vorona, I. P., Okulov, S. M., Baran, N. P. (2002) 13C hyperfine interactions of CO_2^- in irradiated tooth enamel as studied by EPR. *Applied Radiation and Isotopes* **56**, 815-819.

Joannes-Boyau, R., Grün, R. (2009) Thermal behavior of orientated and non-orientated CO2- radicals in tooth enamel. *Radiation Measurements* **44**, 505-511.

Joannes-Boyau, R., Bodin, T., Grün, R. (submitted) Decomposition of the angular ESR spectra of fossil tooth enamel fragments. *Radiation Measurements*

Joannes-Boyau, R., Grün, R., Bodin, T. (in press) Decomposition of the laboratory gamma irradiation component of angular ESR spectra of fossil tooth enamel fragments. *Applied Radiation and Isotopes*

Kirkpatrick, S., Gelatt, C.D., Vecchi, M.P. (1983) Optimization by simulated annealing. *Science* **220**, 671-680.

Liidja, G., Past, J., Puskar, J., Lippmaa, E. (1996) Paramagnetic resonance in tooth enamel created by ultraviolet light. *Applied Radiation and Isotopes* **47**, 785-788.

Metropolis, N., Rosenbluth, A.W., Rosenbluth, M.N., Teller, A.H., Teller, E. (1953) Equations of state calculations by fast computing machines. *Journal of Chemical Physics* **21**, 1087-1092.

Mosegaard, K., Sambridge, M. (2002) Monte Carlo analysis of inverse problems. *Inverse Problems* **18**, 79161-79162.

Nilsson, J., Lund, E., Lund, A. (2001) The effects of UV-irradiation on the ESR-dosimetry of tooth enamel. *Applied Radiation and Isotopes* **54**, 131-139.

Porat, N., Zhou, L.P., Chazan, M., Noy, T., Horwitz L.K. (1999) Dating the lower Paleolithic open-air site of Holon, Israel by luminescence and ESR technologies. *Quaternary Research* **51**, 328–341.

Romanyuhka, A.A., Regulla, D., Vasilenko, E., Wieser, A. (1994) South Ural nuclear workers: comparison of individual doses from retrospective EPR dosimetry and operational personal monitoring. *Applied Radiation and Isotopes* **45**, 1195–1199.

Rudko, V.V., Vorona, I.P., Baran, N.P., Ishchenko, S.S. (2007) γ- and UV-induced radicals in tooth enamel. *Radiation Measurements* **42**, 1181-1184.

Schramm, D.U., Rossi, A.M. (2000) Electron spin resonance (ESR) studies of CO−2 radicals in irradiated A and B-type carbonate-containing apatites. *Applied Radiation and Isotopes* **52**, 1085-1091.

Vorona, I.P., Baran, N.P., Ishchenko, S.S., Rudko, V.V. (2007) Separation of the contributions from γ- and UV-radiation to the EPR spectra of tooth enamel plates. *Applied Radiation and Isotopes* **65**, 553-556.

Reviewer
Jean-Jacques Bahain